

## Stacking-dependent optical spectra and many-electron effects in bilayer graphene

Zhifan Chen and Xiao-Qian Wang\*

*Department of Physics and Center for Functional Nanoscale Materials, Clark Atlanta University, Atlanta, Georgia 30314, USA*

(Received 28 December 2010; published 10 February 2011)

We have studied the electronic and optical properties of twisted bilayer graphene using the first-principles *GW*-Bethe-Salpeter equation approach. The optical absorption spectrum of twisted-bilayer graphene is analogous to that of graphene, which is attributed to the characteristic dispersion of Dirac fermions and is contrary to the Bernal-stacking bilayer graphene. Many-electron effects play a pivotal role in the optical spectrum and quasiparticle excitations, which yield an enhanced excitonic resonance and an induced renormalization of the Fermi velocity for twisted bilayer graphene. Our results indicate that it is necessary to consider electron-electron and electron-hole interactions simultaneously for describing the corresponding many-electron effects.

DOI: [10.1103/PhysRevB.83.081405](https://doi.org/10.1103/PhysRevB.83.081405)

PACS number(s): 73.22.-f, 72.80.Rj, 75.70.Ak

Graphene, a single layer of an all-carbon hexagonal network, is an emerging material for applications in electronics and photonics.<sup>1-6</sup> As a truly two-dimensional system and a zero-gap semiconductor in which the low-energy excitation is characteristic of massless Dirac fermions, graphene possesses a number of intriguing electronic properties, such as quantization of the conductivity,<sup>1</sup> tunable carrier type and density,<sup>2</sup> exceptionally high carrier mobility,<sup>3</sup> and quantum Hall effect (QHE).<sup>7</sup> These phenomena, particularly the half-integer QHE, have generated a revived interest in the development of novel ideas in many-body physics such as chiral Luttinger liquids,<sup>8</sup> composite fermions,<sup>9</sup> and topological insulators.<sup>10</sup>

Bringing graphene up to the level of technologically relevant material, however, depends on improved understanding and control of the structural and electronic properties. Recent theoretical and experimental works have demonstrated that bilayer graphene can have a tunable gap via chemical doping or by applying an external gate voltage.<sup>11,12</sup> In Bernal-stacking bilayer graphene, the low-energy excitations are instead one of the characteristics of massive chiral fermions.<sup>13,14</sup> In lieu of the increasing amount of experimental and theoretical studies of bilayer graphene transistors,<sup>15</sup> the exploration of various modified bilayer systems could play a crucial role in future nanoelectronics applications.

In addition to the Bernal-stacking bilayer graphene (BLG), the twisted bilayer graphene (TBG) has attracted a great deal of attention recently. Experimental work<sup>16</sup> revealed that the optical conductivities of TBG samples are frequency dependent in the visible light range, contrary to the frequency-independent ones of single-layer graphene (SLG) and BLG. On the other hand, recent experimental work indicated that typically there exists orientational disorder in carbon-face SiC epitaxial multilayer samples.<sup>17</sup> The energy bands of commensurate twisted multilayers disperse nearly linearly with momentum in the proximity of the Dirac point. As such, twisted multilayers are poised to provide a promising platform for applications. The present work is thus motivated primarily by the need to attain a thorough understanding of stacking-dependent optical spectra and many-electron effects.

From a theoretical perspective, a fundamental understanding of stacking-dependent photoexcitations and quasiparticle excitations of bilayer graphene is still lacking. There were only limited *ab initio* band-structure calculations within the

local-density approximation (LDA) or generalized-gradient approximation (GGA) of the density-functional theory (DFT) for TBG.<sup>16-20</sup> The LDA and GGA are known to fail in describing electron-hole (*e-h*) and electron-electron (*e-e*) interactions that are responsible for the formation of excitons and the quasiparticle excitations. A first-principles study of the quasiparticles and their interaction with light in bilayer graphene need to include those effects. In this regard, the *GW*-Bethe-Salpeter equation (*GW*-BSE) approach stands for one of the state-of-the-art theories beyond DFT.<sup>21,22</sup>

Our first-principles calculations of the optical excitation for the BLG and TBG were performed using the many-body *GW*-BSE perturbation correction to DFT results. The geometry optimization for the BLG and TBG was obtained by performing a density-functional calculation within LDA. The Vosko-Wilk-Nusair<sup>23</sup> exchange-correlation function was used for the LDA calculation. The reason for choosing LDA as the starting point is attributed to the fact that GGA leads to weak bonding between graphene layers and yields excessively large values of bilayer distance. By contrast, the LDA calculation gives rise to reasonable bilayer distances.<sup>15</sup>

Depicted in Fig. 1 are optimized conformations for BLG and the TBG with an orientation angle of  $\theta = 21.8^\circ$ , respectively. The corresponding rhombus unit cell consists of four and 28 carbon atoms, respectively. A large enough supercell of 18 Å in the direction perpendicular to TBG or BLG was employed in order to eliminate the interaction between replicas. A method<sup>24</sup> to remove the long-range tail of Coulomb potentials has been used also in the calculation. The optimization of atomic positions were proceeded until the change in energy was less than  $2 \times 10^{-5}$  eV and the forces are less than  $5 \times 10^{-3}$  eV/Å. Troullier-Martins norm-conserving pseudopotentials and a kinetic energy cutoff of 435 eV were employed in solving the Kohn-Sham equation. Monkharst-Pack meshes of  $32 \times 32 \times 1$  were used for BLG and SLG and  $6 \times 6 \times 1$  for TBG. The fully relaxed bilayer distance is 3.17 and 3.47 Å for BLG and TBG of  $21.8^\circ$ , respectively.

The  $\theta = 21.8^\circ$  rotation between adjacent graphene layers is the smallest possible commensuration, and thus serves as a prototypical stacking fault in twisted multilayers.<sup>17</sup> We show in Fig. 2 the calculated band structures for BLG and TBG of  $\theta = 21.8^\circ$ , respectively. As seen in Fig. 2, the  $\pi$ -electron dispersion in the valence and conduction bands of BLG splits

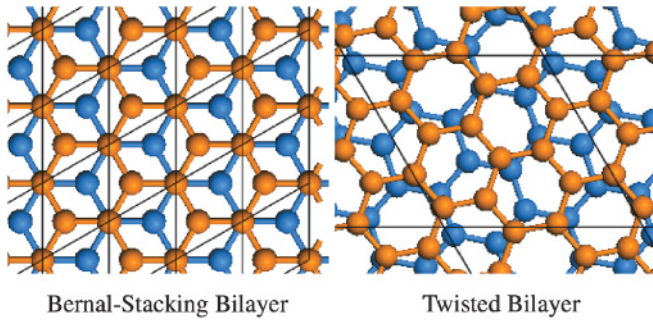


FIG. 1. (Color online) Top view of the optimized conformations of Bernal-stacking bilayer and a twisted bilayer graphene with an orientation angle of  $\theta = 21.8^\circ$ , respectively.

into two parabolic branches near  $K$ , the Dirac point. The band splitting of  $\sim 0.4$  eV is attributed to a strong interlayer coupling associated with the Bernal stacking. By contrast, the corresponding bands of commensurate TBG preserve the linear dispersion around the Dirac point as in graphene. For BLG and TBG, the predominant energy span between  $\pi$  and  $\pi^*$  bands at  $M$  is  $\sim 4$  eV, which is characteristic of graphene as well. However, the expanded unit cell of commensurate TBG leads to a reduced Brillouin zone with band folding, which prunes the range of linear dispersion, along with a stacking-dependent decrease of the minimal energy span between  $\pi$  and  $\pi^*$  bands at  $M$ . Because the band split at  $M$  for commensurate TBG falls into the visible light range ( $\sim 2.8$  eV for TBG of  $\theta = 21.8^\circ$ ), there exists a profound modification to the corresponding light absorption behavior.<sup>16</sup>

The quasiparticle corrections to the LDA eigenvalues were evaluated by using a one-shot approach referred to as the  $G_0W_0$  approximation. In this approach the electron self-energy,  $\Sigma$ , is calculated by summing up ring polarization diagrams to the lowest order in the screened Coulomb interaction, through a product of the one-electron Green's function  $G_0$  and the dynamical screened Coulomb interaction  $W_0$  as  $\Sigma = iG_0W_0$ . The LDA eigenvalues and eigenfunctions were used to

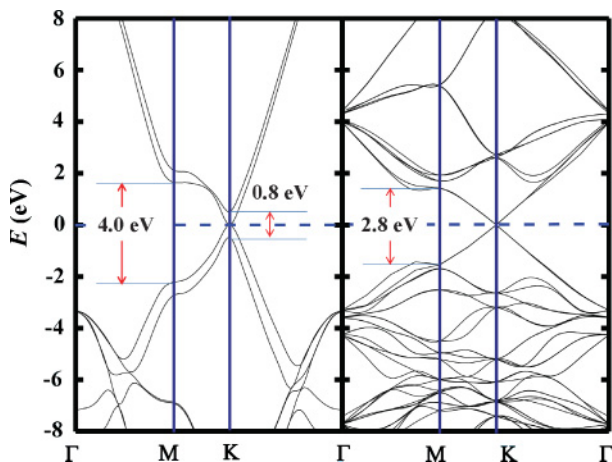


FIG. 2. (Color online) Calculated band structures for BLG (left-hand panel) and TBG with an orientation angle of  $\theta = 21.8^\circ$  (right-hand panel), respectively.  $\Gamma = (0,0)$ ,  $K = (\pi/3a, 2\pi/3a)$ ,  $M = (0, \pi/2a)$ , where  $a = 2.46$  and  $6.50$  Å for BLG and TBG of  $21.8^\circ$ , respectively.

construct the one-electron Green's function  $G_0$ . The screened Coulomb interaction was calculated within the random-phase approximation (RPA) and the self-energy was evaluated by the plasmon-pole approximation.<sup>25</sup> It is worth pointing out that the self-energy is evaluated by the  $GW$  method rather than the RPA as the latter is not justified for Dirac fermions near the Dirac point.<sup>26</sup>

On the basis of quasielectron and quasihole states, the absorption spectrum was extracted by solving the BSE.<sup>25</sup> In the present calculation we used the so-called Tamm-Dancoff approximation (TDA).<sup>27</sup> In this approximation, only positive energy  $e$ - $h$  pairs and the resonance of the BSE are considered, whereas the coupling between the BSE and the  $e$ - $h$  antipairs is neglected. The advantage of the TDA is that the non-Hermitian BSE reduces to an Hermitian one that can be solved by an efficient iterative method.

Summarized in Fig. 3 are the calculated in-plane absorption spectra using  $GW$ -BSE along with those using RPA and  $GW$ -RPA for SLG, TBG of  $\theta = 21.8^\circ$ , and BLG, respectively. The optical absorption spectra can be divided in two regions: a low-energy region up to 5 eV that is attributed from transitions among  $\pi$  and  $\pi^*$  bands, whereas the region beyond 10 eV is originated from  $\sigma$  and  $\sigma^*$  transitions. While RPA can be regarded as the result at the DFT level,  $GW$ -RPA includes  $e$ - $e$  interactions, and  $GW$ -BSE goes beyond RPA by including  $e$ - $e$  and  $e$ - $h$  interactions.

Our calculated optical spectra are in good conformity with available calculation results in the literature.<sup>21,22</sup> Specifically, a common spectroscopic attribute of these systems is the existence of a prominent  $\pi$ - $\pi^*$  RPA peak at  $\sim 3.9$  eV,<sup>16,22</sup> and  $GW$ -RPA results exhibit overall blueshifts, and  $GW$ -BSE ones yield overall smaller blue-shifts than the corresponding  $GW$ -RPA absorption peaks.<sup>21</sup> Furthermore, it is readily observable from Fig. 3 that there exists a RPA absorption peak at 0.8 eV for BLG and a band-folding-induced RPA feature at  $\sim 2.9$  eV for TBG of  $\theta = 21.8^\circ$ .

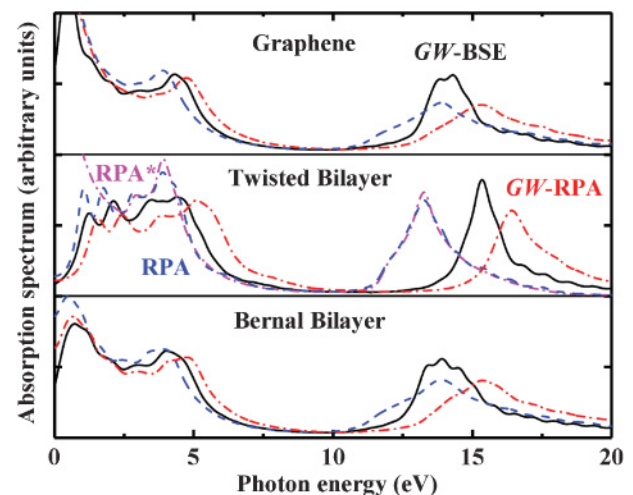


FIG. 3. (Color online) Calculated absorption spectra using  $GW$ -BSE (black solid lines), RPA (blue dashed line), and  $GW$ -RPA (red dashed-dotted lines) for TBG with an orientation angle of  $\theta = 21.8^\circ$  (middle panel), BLG (bottom panel), and SLG (top panel), respectively. The magenta dashed-dotted line illustrates RPA\* results using  $k$ -point meshes of  $24 \times 24 \times 1$  for TBG.

The RPA absorption peak at 0.8 eV for BLG is attributed to the  $\pi$ - $\pi^*$  transition at the Dirac point, which is correlated to interlayer-coupling-induced band splitting. Whereas the inclusion of  $e$ - $e$  GW effects yields a blueshift of the characteristic peak,<sup>21,22</sup> the inclusion of  $e$ - $h$  interaction effects via BSE leads to a redshift. The GW-BSE result has a compound blueshift of 0.1 eV for BLG over the RPA one, implying that the self-energy corrections and excitonic effects nearly cancel each other out for this characteristic.

A few remarks are in order. (i) With regard to the excitonic resonances associated with the  $\sigma$  and  $\sigma^*$  transitions,<sup>22</sup> our GW-BSE results indicate strongly enhanced excitonic effects in that the GW-RPA peaks at 13.9, 13.9, and 13.2 eV for SLG, TBG of  $\theta = 21.8^\circ$ , and BLG redshift to 15.3, 15.4, and 16.4 eV for GW-RPA, and have a smaller redshift to 14.2, 14.0, and 15.4 eV for GW-BSE, respectively. For SLG and BLG the excitonic effects are nearly canceled with the  $e$ - $e$  effect. By contrast, there are band-folding-induced increases in the  $\sigma$  and  $\sigma^*$  electronic density of states that lead to a stronger  $e$ - $e$  rectification and residual blueshift of the corresponding GW-BSE peak for TBG. It is worth noting that these results are qualitatively distinct from those obtained from BSE calculations alone,<sup>22</sup> indicating the importance of including  $e$ - $e$  and  $e$ - $h$  interactions simultaneously. (ii) Significant excitonic effects are found in the optical absorption spectra as the prominent RPA peaks  $\sim 3.9$  eV have blueshifts of  $\sim 0.8$ – $1.2$  eV using GW-RPA, and smaller blueshifts of  $\sim 0.1$ – $0.5$  eV using GW-BSE. Our GW-BSE results are in good conformity with previous ones<sup>21</sup> for SLG. (iii) The RPA 2.8-eV feature for TBG of  $\theta = 21.8^\circ$  is connected to the band-folding-induced gap near  $M$ .<sup>16</sup> Our GW-BSE results also demonstrate important excitonic effects for the band-folding effects in that there exists a  $\sim 0.6$  eV blueshift for the characteristic GW-RPA peak. While we limit ourselves in investigating TBG of  $\theta = 21.8^\circ$  largely owing to computational considerations, we believe that the same effects should be observable for other TBG samples, which leads to important rectifications to the band-folding-induced frequency-dependent optical conductances.<sup>16</sup>

A natural question arises regarding the clarification of many-electron effects for in-plane and interlayer interactions of TBG. To understand this it is instructive to examine various peaks related to  $\pi$  and  $\pi^*$  transitions as shown in Fig. 3 and thoroughly test the convergence of the results. For GW-BSE calculations, the low-energy peaks are very sensitive to the  $k$ -point meshes used, and the convergence of high-energy peaks is mainly determined by the energy cutoffs employed. A

careful examination of the kinetic energy cutoffs indicates that the high-energy portion of the optical spectra is reliable. For the low-energy part of the TBG of  $\theta = 21.8^\circ$ , it appears that the lowest two peaks at 1.1 and 1.8 eV are the artifacts of a small set of  $k$ -point meshes ( $6 \times 6 \times 1$ ) employed. As shown in Fig. 3, the two peaks disappear after increasing the  $k$ -point meshes to  $24 \times 24 \times 1$ . In the energy region larger than 2.5 eV the results are virtually identical to those using a  $6 \times 6 \times 1$  mesh. In fact, the optical response of TBG of  $\theta = 21.8^\circ$  closely resembles that of graphene, indicating a very weak interlayer coupling effect in the vicinity of the Dirac cone.

By way of contrast to BLG in which there is a paucity of a blueshift for the corresponding low-energy optical responses, the low-energy RPA parts have an overall blueshift using GW-BSE. The overall blue shift for  $\pi$  and  $\pi^*$  transitions suggests a renormalization of the Fermi velocity  $v_F$  of the Dirac cones. Because the Fermi velocity of the Dirac cones is the same for graphene and TBG of  $\theta = 21.8^\circ$  at the DFT level,<sup>20</sup> the renormalization of the Fermi velocity is entirely owing to many-electron effects.<sup>26</sup> It is worth pointing out that such a renormalization of the Fermi velocity is definitely distinctive to that for small commensurate angle TBG systems, which is simply owing to band-folding and flat-band effects.<sup>20</sup>

In summary, we have studied the electronic excitations and optical spectra of twisted bilayer graphene from first-principles approaches including both  $e$ - $e$  self-energy corrections and  $e$ - $h$  correlations. Our attention is directed to the stacking-dependent coupling between twisted layers. Our GW-BSE results indicate that there exists a profound difference in electronic properties between BLG and TBG. In TBG, the decoupling of Dirac points in neighboring layers is advantageous in accessing two-dimensional physics in a family of three-dimensional materials.<sup>17</sup> The strongly enhanced excitonic effect is shown to manifest itself through a strong excitonic resonances owing to the interlayer coupling. Our findings shed important light on the nature of many-body effects in twisted layers and assert advantages of the relevant twisted multilayers as materials for future nanoelectronic devices.

This work was supported by the National Science Foundation (Grant No. DMR-0934142, and through TeraGrid resources provided by NCSA Lincoln and Abe systems under Grant No. PHY100041), Army Research Office (Grant No. W911NF-06-1-0442), and Air Force Office of Scientific Research (Grant No. FA9550-10-1-0254). We have used ABINIT and YAMBO codes in the calculations.

\*xwang@cau.edu

<sup>1</sup>K. S. Novoselov, A. K. Geim, S. V. Morozov, D. Jiang, M. I. Katsnelson, I. V. Grigorieva, S. V. Dubonos, and A. A. Firsov, *Nature (London)* **438**, 197 (2005).

<sup>2</sup>C. Berger, Z. M. Song, Xuebin Li, Xiaosong Wu, Nate Brown, Cécile Naud, Didier Mayou, Tianbo Li, Joanna Hass, Alexei N. Marchenkov, Edward H. Conard, Phillip N. First, and Walt A. de Heer, *Science* **312**, 1191 (2006).

<sup>3</sup>Y. Zhang, Z. Jiang, J. P. Small, M. S. Purewal, Y.-W. Tan, M. Fazlollahi, J. D. Chudow, J. A. Jaszczak, H. L. Stormer, and P. Kim, *Phys. Rev. Lett.* **96**, 136806 (2006).

<sup>4</sup>A. K. Geim, S. V. Morozov, E. W. Hill, P. Blake, M. I. Katsnelson, and K. S. Novoselov, *Nat. Mater.* **6**, 183 (2007).

<sup>5</sup>X. Wang, L. Zhi, and K. Mullen, *Nano Lett.* **8**, 323 (2008).

<sup>6</sup>S. Gilje, S. Han, M. Wang, K. L. Wang, and R. B. Kaner, *Nano Lett.* **7**, 3394 (2007).

- <sup>7</sup>Y. Zhang, Y. W. Tan, H. L. Stormer, and P. Kim, *Nature (London)* **438**, 201 (2005).
- <sup>8</sup>M. Killi, T. C. Wei, I. Affleck, and A. Paramekanti, *Phys. Rev. Lett.* **104**, 216406 (2010).
- <sup>9</sup>C. Töke, P. E. Lammert, V. H. Crespi, and J. K. Jain, *Phys. Rev. B* **74**, 235417 (2006).
- <sup>10</sup>P. M. Ostrovsky, I. V. Gornyi, and A. D. Mirlin, *Phys. Rev. Lett.* **105**, 036803 (2010).
- <sup>11</sup>N. A. H. Castro, F. Guinea, N. M. R. Peres, K. S. Novoselov, and A. K. Geim, *Rev. Mod. Phys.* **81**, 109 (2009).
- <sup>12</sup>E. McCann and V. I. Fal'ko, *Phys. Rev. Lett.* **96**, 086805 (2006).
- <sup>13</sup>E. V. Castro, K. S. Novoselov, S. V. Morozov, N. M. R. Peres, J. M. B. Lopes dos Santos, Johan Nilsson, F. Guinea, A. K. Geim, and A. H. Castro Neto, *Phys. Rev. Lett.* **99**, 216802 (2007).
- <sup>14</sup>J. Nilsson, A. H. Castro Neto, F. Guinea, and N. M. R. Peres, *Phys. Rev. B* **76**, 165416 (2007).
- <sup>15</sup>D. K. Samarakoon and X.-Q. Wang, *ACS Nano* **4**, 4126 (2010).
- <sup>16</sup>Y. Wang, Z. Ni, Lei Liu, Yanhong Liu, Chunxiao Cong, Ting Yu, Xiaojun Wang, Dezhen Shen, and Zexiang Shen, *ACS Nano* **4**, 4074 (2010).
- <sup>17</sup>M. Sprinkle, D. Siegel, Y. Hu, J. Hicks, A. Tejada, A. Taleb-Ibrahimi, P. Le Fèvre, F. Bertran, S. Vizzini, H. Enriquez, S. Chiang, P. Soukiassian, C. Berger, W. A. de Heer, A. Lanzara, and E. H. Conrad, *Phys. Rev. Lett.* **103**, 226803 (2009).
- <sup>18</sup>Z.-H. Ni, L. Liu, Y.-Y. Wang, Z. Zheng, L.-J. Li, T. Yu, and Z. Shen, *Phys. Rev. B* **80**, 125404 (2009).
- <sup>19</sup>S. Shallcross, S. Sharma, and O. A. Pankratov, *Phys. Rev. Lett.* **101**, 056803 (2008).
- <sup>20</sup>E. Suárez Morell, J. D. Correa, P. Vargas, M. Pacheco, and Z. Barticevic, *Phys. Rev. B* **82**, 121407(R) (2010).
- <sup>21</sup>L. Yang, J. Deslippe, C.-H. Park, M. L. Cohen, and S. G. Louie, *Phys. Rev. Lett.* **103**, 186802 (2009).
- <sup>22</sup>P. E. Trevisanutto, M. Holzmann, M. Côté, and V. Olevano, *Phys. Rev. B* **81**, 121405(R) (2010).
- <sup>23</sup>S. J. Vosko, L. Wilk, and M. Nusair, *Can. J. Phys.* **58**, 1200 (1980).
- <sup>24</sup>C. A. Rozzi, D. Varsano, A. Marini, E. K. U. Gross, and A. Rubio, *Phys. Rev. B* **73**, 205119 (2006).
- <sup>25</sup>A. Marini, C. Hogan, M. Gruning, and D. Varsano, *Computer. Phys. Commun.* **180**, 1392 (2009).
- <sup>26</sup>E. G. Mishchenko, *Phys. Rev. Lett.* **98**, 216801 (2007).
- <sup>27</sup>M. Grüning, A. Marini, and X. Gonze, *Nano Lett.* **9**, 2820 (2009).